processes

MDPI

Article

Stick–Slip Characteristics of Drill Strings and the Related Drilling Parameters Optimization

Chao Wang [1], Wenbo Chen [1], Zhe Wu [2,*], Jun Li [2] and Gonghui Liu [3]

[1] School of Mechanical Engineering, Yangtze University, Jingzhou 434023, China; cw_paper@163.com (C.W.); cwb_paper@163.com (W.C.)
[2] College of Petroleum Engineering, China University of Petroleum-Beijing, Beijing 102249, China; lijun446@vip.163.com
[3] Beijing University of Technology, Beijing 100124, China; lgh_1029@163.com
* Correspondence: zhewu_paper@163.com

Abstract: To eliminate or reduce stick–slip vibration in torsional vibration of the drilling string and improve the rate of penetration (ROP), a stick–slip vibration model of the drilling string considering the ROP was established based on the multidimensional torsional vibration model of the drilling string. The model was verified by simulation analysis. The characteristics of the drilling string stick–slip vibration in the three stages of stationary, slip, and stick were analyzed. This paper investigated the influence of rotary torque, rotary speed, and weight on bit (WOB) on stick–slip vibrations in the drill string. Based on this, the relationship between the drilling parameters and ROP was established. Drilling parameter optimization was completed for soft, medium-hard, and hard formations. Results showed that appropriately increasing torque and decreasing WOB can reduce or even eliminate stick–slip vibrations in the drill string and increase the ROP. The parameter optimization increased the ROP by 11.5% for the soft formation, 13.7% for the medium-hard formation, and 14.3% for the hard formation. The established drill string stick–slip vibration model provides theoretical guidance for optimizing drilling parameters in different formations.

Keywords: drill string; stick–slip vibration; drilling parameter; optimization

Citation: Wang, C.; Chen, W.; Wu, Z.; Li, J.; Liu, G. Stick–Slip Characteristics of Drill Strings and the Related Drilling Parameters Optimization. *Processes* **2023**, *11*, 2783. https://doi.org/10.3390/pr11092783

Academic Editors: Tianshou Ma and Yuqiang Xu

Received: 26 August 2023
Revised: 8 September 2023
Accepted: 14 September 2023
Published: 18 September 2023

1. Introduction

Nowadays, human demand for petroleum resources is increasingly strong. Exploration and drilling/production of oil/gas resources are gradually moving deeper, and formation structures are more complex. The number of complex structured wells such as deep, ultra-deep, and extended-reach wells is increasing, making drilling engineering operations more difficult. During drilling, drill strings vibrate due to formation friction, lithology, and pressure, potentially causing drilling accidents such as premature bit failure, drill string damage, and low ROP.

Drill string vibrations are typically categorized as axial vibration, transverse vibration, and torsional vibration. The coupled vibrations lead to complex behaviors such as bit jumping, stick–slip vibration, and vortex motion. Among these complex behaviors, stick–slip vibration is most harmful. It induces cyclical stress and strain fluctuations in the drill string, accelerating fatigue failure and severely impacting drill string and bit life. Severe stick–slip vibration also causes intense vibration of the rig and derrick, damaging surface equipment and greatly reducing drilling efficiency [1].

Therefore, to improve drilling efficiency and protect equipment, drill string stick–slip vibration characteristics must be analyzed and proper measures taken to reduce or eliminate stick–slip vibration. Researchers discovered stick–slip phenomena in drill strings and conducted in-depth research as early as the 1980s [2]. Many studies on eliminating stick–slip vibration in drill string torsional vibration have laid the foundation for this research. In terms of modeling and analysis, references [2–5] established drill string stick–slip

vibration dynamics models considering various coupling effects, analytically obtained modal characteristics of the complex coupled systems, and laid theoretical foundations for studying the dynamics mechanisms of stick–slip vibrations in drill strings. Reference [6] obtained an analytical expression of the velocity-weakening friction law through a toothed-bit model, revealing the role of bit–rock interactions in the generation of stick–slip vibrations. Reference [7] analyzed the combined torsional stick–slip and lateral whirling vibrations through simplified models, explaining the dynamics mechanisms between different vibration modes. Regarding control strategies, reference [8] proposed an active damping system based on feedback control that effectively suppresses self-excited torsional vibrations of the drill string during drilling by adjusting drive system parameters, expanding the non-vibrating rotary speed range of the drill string. This provided new ideas and references for eliminating nonlinear stick–slip vibrations during drill string rotation. Reference [9] proposed robust control strategies based on model error compensation techniques and constructed cascade and decentralized control schemes. Reference [10] adopted dynamic sliding mode control, established discontinuous torsional dynamics models and dual discontinuous surfaces, achieved rotary speed control of the oilwell drill string, and effectively suppressed self-excited stick–slip vibrations. This provided an important control strategy reference for eliminating stick–slip vibrations in drill strings. Reference [11] designed an improved OSKIL mechanism called D-OSKIL by using axial load as an additional control variable to suppress drill string limit cycles during drilling. This control law rendered the closed-loop system globally asymptotically stable. Simulations verified that stick–slip vibrations can be effectively eliminated without redesigning rotary speed control. Regarding parameter optimization, reference [12] established an oilwell drilling dynamics model, analyzed the self-excited vibration issue at the bottom hole assembly, and proposed key drilling parameter selection guidance to avoid drill string torsional vibrations. This provided new insights into parameter design for eliminating nonlinear stick–slip vibrations during drill string rotation. Reference [13] studied the effects of damping, active control, and interface parameter optimization on stick–slip vibrations. Reference [14] pointed out that bit interface conditions are key factors affecting vibrations. In terms of mechanism theory, reference [15] laid the foundation for drill string torsional vibration research by proposing and validating the stick–slip vibration theory. Reference [16] proposed a new perspective wherein velocity weakening is a system response rather than an intrinsic characteristic. Reference [17] revealed the mechanism of normal and tangential vibrations in stick–slip limit cycles through a two-degrees-of-freedom model. Regarding coupled vibrations, reference [18] avoided self-excited vibrations to suppress stick–slip vibrations. Reference [19] analyzed drill string torsional vibration issues caused by derrick stick–slip motion through establishing a stick–slip vibration model and proposed avoiding large-amplitude vibrations through rotary speed control strategies. Reference [20] proposed a new robust active controller based on the fuzzy sliding mode approach to suppress stick–slip vibration in drill strings and maintain the angular velocity of drill components at desired values. Reference [21] established an axial–lateral–torsion coupling nonlinear model for drill string vibration in ultra-HPHT curved wells considering wellbore constraints, bit–rock interaction, and mud properties. A finite element method was used for the numerical solution. Reference [22] developed a modified integral resonant control scheme with tracking to suppress stick–slip vibrations and achieve the desired drilling velocity in drill strings, showing better performance than sliding mode control. Reference [23] designed an H observer-based controller to estimate and suppress high-frequency stick–slip vibrations in a 10-DOF drill string model, showing better performance than LQG control in handling unstructured perturbations. Reference [24] introduced a new model for analyzing the Anti-Stick–Slip Tool at the drill string's end. This model overcomes the limitations of previous analyses, utilizing two degrees of freedom in the non-activated state and three degrees upon activation.

In summary, the above studies have laid theoretical foundations for this study's drill string stick–slip vibration elimination. However, there has been less systematic

discussion on the stick–slip mechanism and its influencing factors. What is more, less work has focused on combining a stick–slip vibration elimination model and ROP model in order to ensure high ROP and less stick–slip at the same time, especially when drilling in different formations.

This paper establishes and validates a drill string stick–slip vibration behavior model based on the drill string torsional vibration model. It reveals characteristics of stick–slip vibrations in different positions along the drill strings and analyzes influencing factors based on the simulation results. With one-time integration and two-time integration, the stick–slip angular velocity and angular displacement along the drill strings can be achieved, which can further reveal the stick–slip mechanization and characteristics. To reduce stick–slip and, in turn, increase ROP, this paper carries out drilling parameter optimization for soft, medium-hard, and hard formations by combining an ROP calculation model and stick–slip model. The optimization method generates preferred drilling parameter ranges applicable to different formations, improving mechanical ROP under relatively stable torsional vibrations. This has very important guiding significance for on-site drilling operation safety.

2. Drill String Stick–Slip Vibration and Drilling Parameter Optimization

2.1. The Multidimensional Drill String Torsional Vibration Model

In actual drilling, surface-applied torque on the rotary drives continuous rotation of the drill pipe, drill collar, drill bit, and other tools. Meanwhile, under the drill bit's WOB, the bit cuts rock to achieve penetration. Based on extensive research worldwide, reasonable simplification and assumptions were made for drill string torsional vibrations considering differences in the mechanical properties of various drill pipes and drill collars. Thus, a multidimensional drill string torsional vibration model was constructed.

This model views the rotary table, m drill pipes, n drill collars, drill bit, etc., as lumped masses; other tools are viewed as springs with torsional stiffness and viscous damping. Under actual conditions, the following assumptions are made:

(1) The research object is a vertical well;
(2) The drill string is simplified into lumped masses including the rotary table, m drill pipes, n drill collars, and the bit;
(3) BHA is equivalent to springs and viscous damping;
(4) Overall stick–slip behavior of the drill string is approximated by stick–slip at the bit.

Figure 1 shows the multidimensional drill string torsional-vibration-model-based rotary table, drill pipe 1…n, drill collars 1…n, and drill bit. J_{r}, J_{p1}, J_{pm}, J_{c1}, J_{cl}, and J_{b} represent the rotational inertias of the rotary table, drill pipe 1, drill pipe n, drill collar 1, drill collar n, and drill bit, respectively, kg·m^2. $\ddot{\varphi}_r$, $\ddot{\varphi}_{p1}$, $\ddot{\varphi}_{pm}$, $\ddot{\varphi}_{c1}$, $\ddot{\varphi}_{cn}$, and $\ddot{\varphi}_b$ represent the angular accelerations of the rotary table, drill pipe 1, drill pipe m, drill collar 1, drill collar n, and drill bit, respectively, rad/s^2. $\dot{\varphi}_r$, $\dot{\varphi}_{p1}$, $\dot{\varphi}_{pm}$, $\dot{\varphi}_{c1}$, $\dot{\varphi}_{cn}$, and $\dot{\varphi}_b$ represent the angular velocities of the rotary table, drill pipe 1, drill pipe m, drill collar 1, drill collar n, and drill bit, respectively, rad/s. φ_r, φ_{p1}, φ_{pm}, φ_{c1}, and φ_{cn} represent the angular displacements of the rotary table, drill pipe 1, drill pipe m, drill collar 1, and drill collar n, respectively, rad. c_{r}, c_{rp}, c_{p1}, $c_{\mathrm{pm\text{-}1}}$, c_{pc}, c_{c1}, $c_{\mathrm{cn\text{-}1}}$, c_{cb}, and c_{b} represent the damping coefficients of the rotary table, between the rotary table and drill pipe, between drill pipes, between the drill pipe and collar, between drill collars, between the drill collar and bit, and of the drill bit, respectively, (N·m·s)/rad. T_{m}, T_{e}, T_{ar}, T_{f}, T_{ab}, T_{fb}, T_{sb}, and T_{cb} represent the torque of the rotary table, torque transferred to the drill bit, viscous torque of the rotary table, friction torque of the drill bit, viscous torque of the drill bit, dry friction torque of the drill bit, maximum static friction torque, and Coulomb friction torque, respectively, N·m. k_{rp}, k_{p1}, $k_{\mathrm{pm\text{-}1}}$, k_{pc}, k_{c1}, $k_{\mathrm{cn\text{-}1}}$, and k_{cb} represent the stiffness coefficients between the rotary table and drill pipe, between drill pipes, between the drill pipe and collar, between drill collars, and between the drill collar and bit, respectively, N·m/rad. D_{v} represents the boundary layer thickness, rad/s. R_{b} represents the drill bit radius, m. W_{ob} represents the weight on bit, N.

μ_{cb}, μ_{sb}, and γ_b represent the Coulomb friction coefficient, static friction coefficient, and Stribeck constant, respectively. T_m can be obtained by the following formula:

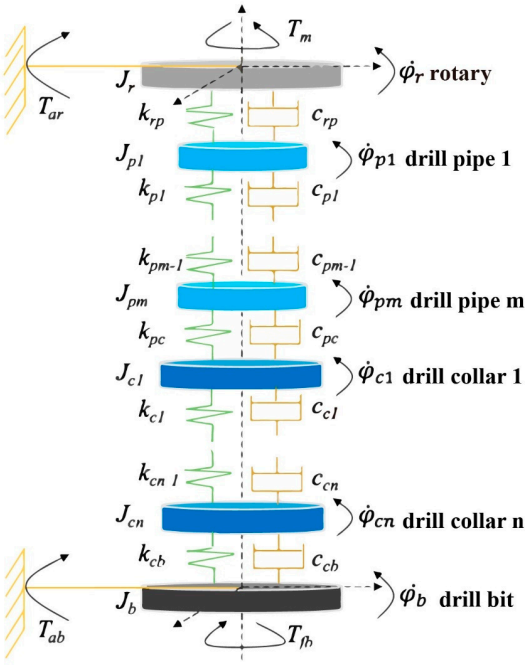

Figure 1. The multidimensional drill string torsional vibration model.

$$T_m = \frac{30P}{\pi n}\eta \tag{1}$$

where P is the rotary table power, W; η is the transmission efficiency, dimensionless; n is the rotation speed of rotary, rad/s. The fluid sticking torque Tar at the rotary table is obtained by the following formula:

$$T_{ar} = -c_r\dot{\varphi}_r \tag{2}$$

where c_r is the rotary table viscous damping coefficient, (N·m·s)/rad. The drill bit is mainly under two torques: the torque T_e transferred from the drill collar to the bit and the friction torque T_f at the bit. The friction torque T_f includes the fluid sticking torque T_{ab} and the dry friction torque T_{fb} between the bit and the rock, which can be expressed as:

$$T_f = \begin{cases} R_b W_{ob}\left[\mu_{cb} + (\mu_{sb} - \mu_{cb})e^{\gamma_b\dot{\varphi}_b}\right] - c_b\dot{\varphi}_b, & \dot{\varphi}_b \le -D_v \\ -f_e, & |\dot{\varphi}_b| < D_v and |T_e| < T_{sb} \\ f_s(-sgn(f_e)), & |\dot{\varphi}_b| < D_v and |T_e| \ge T_{sb} \\ -R_b W_{ob}\left[\mu_{cb} + (\mu_{sb} - \mu_{cb})e^{-\gamma_b\dot{\varphi}_b}\right] - c_b\dot{\varphi}_b, & \dot{\varphi}_b \ge D_v \end{cases} \tag{3}$$

Here, the maximum static friction torque can be obtained by:

$$T_{sb} = \mu_{sb} R_b W_{ob} \tag{4}$$

where μ_{sb} is the drill bit coefficient of maximum static friction, dimensionless; R_b is the bit radius, m; W_{ob} is the WOB, N. Force analysis was performed on the rotary table, m drill pipes, n drill collars, and drill bit separately. Then, based on the law of rotation, the following dynamics equilibrium equations were established [25,26]:

$$\begin{cases} J_r\ddot{\varphi}_r + c_{rp}\left(\dot{\varphi}_r - \dot{\varphi}_{p1}\right) + k_{rp}\left(\varphi_r - \varphi_{p1}\right) = T_m + T_{ar} \\ J_{p1}\ddot{\varphi}_{p1} + c_{p1}\left(\dot{\varphi}_{p1} - \dot{\varphi}_{p2}\right) + k_{p1}\left(\varphi_{p1} - \varphi_{p2}\right) \\ \qquad = c_{rp}\left(\dot{\varphi}_r - \dot{\varphi}_{p1}\right) + k_{rp}\left(\varphi_r - \varphi_{p1}\right) \\ \cdot \\ J_{pm}\ddot{\varphi}_{pm} + c_{pc}\left(\dot{\varphi}_{pm} - \dot{\varphi}_{c1}\right) + k_{pc}\left(\varphi_{pm} - \varphi_{c1}\right) \\ = c_{pm-1}\left(\dot{\varphi}_{pm-1} - \dot{\varphi}_{pm}\right) + k_{pm-1}\left(\varphi_{pm-1} - \varphi_{pm}\right) \\ J_{c1}\ddot{\varphi}_{c1} + c_{c1}\left(\dot{\varphi}_{c1} - \dot{\varphi}_{c2}\right) + k_{c1}\left(\varphi_{c1} - \varphi_{c2}\right) \\ \qquad = c_{pc}\left(\dot{\varphi}_{pm} - \dot{\varphi}_{c1}\right) + k_{pc}\left(\varphi_{pm} - \varphi_{c1}\right) \\ \cdot \\ J_{cn}\ddot{\varphi}_{cn} + c_{cb}\left(\dot{\varphi}_{cn} - \dot{\varphi}_b\right) + k_{cb}\left(\varphi_{cn} - \varphi_b\right) \\ \quad = c_{cn-1}\left(\dot{\varphi}_{cn-1} - \dot{\varphi}_{cn}\right) + k_{cn-1}\left(\varphi_{cn-1} - \varphi_{cn}\right) \\ J_b\ddot{\varphi}_b = c_{cb}\left(\dot{\varphi}_{cn} - \dot{\varphi}_b\right) + k_{cb}\left(\varphi_{cn} - \varphi_b\right) + T_f \end{cases} \tag{5}$$

2.2. Drilling Parameters Optimization Based on Drill String Stick–Slip Torsional Vibration

The relationship between drilling parameters and ROP is established. With the goals of vibration reduction/elimination and increased ROP, optimization of drilling parameters such as torque and WOB is completed. This can eliminate stick–slip vibrations and increase ROP simultaneously. This study uses the drill string torsional vibration model and ROP equations to establish the relationship between torque, WOB, and ROP. Combining measured field data and geological data can yield the ROP. The ROP equation is as follows [27]:

$$v_{pc} = K_R(W - M)n^{\lambda}\frac{1}{1 + C_2 h}C_p C_h \tag{6}$$

Here, v_{pc} is the ROP, m/h; W is the WOB, kN; n is the rotate speed, r/min; K_R is the formation drillability coefficient; M is the threshold weight, kN; λ is the rotate speed index; C_2 is the tooth wear coefficient; C_p is the pressure difference influence coefficient; C_h is the water purification coefficient; h is the tooth wear.

Figure 2 is a block diagram of drill string stick–slip vibration drilling parameter optimization. Rotary table torque T_m and WOB W are input. First, the angular rate w of the drill bit can be obtained through the stick–slip vibration model to determine vibration intensity. Second, the rotate speed n of the drill bit can be obtained through the stick–slip vibration model. By combining with WOB W, the ROP v can be obtained. Finally, with the goals of eliminating stick–slip vibration and increasing ROP, the optimal solutions for WOB and rotary table torque can be obtained.

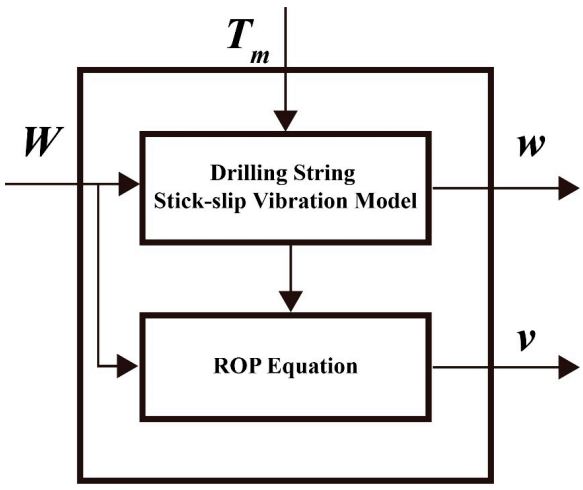

Figure 2. Block diagram of drilling string stick–slip vibration drilling parameter optimization.

3. Stick–Slip Model Validation and Influencing Factors Analysis

3.1. Validation of Stick–Slip Vibration Model

Based on [18], the basic simulation parameters of the drill string stick–slip vibration model are set as shown in Table 1. The simulation time is from 0 to 100 s.

Table 1. Model simulation parameter table.

Parameter Description	Parameter Symbol	Parameter Value
turning inertia of the rotary	J_r	930 kg·m^2
turning inertia of the drill pipe	J_p	2782.25 kg·m^2
turning inertia of the drill collar	J_c	750 kg·m^2
turning inertia of the drill bit	J_b	471.97 kg·m^2
equivalent stiffness coefficient between the rotary and drill pipe	k_{rp}	698.06 N·m/rad
equivalent stiffness coefficient between the drill pipe and drill collar	k_{pc}	1080 N·m/rad
equivalent stiffness coefficient between the drill collar and drill bit	k_{cb}	907.48 N·m/rad
damping coefficient of rotary	c_r	425 N·m/rad
equivalent damping coefficient between the rotary and drill pipe	c_{rp}	139.61 N·m/rad
equivalent damping coefficient between the drill pipe and drill collar	c_{pc}	190 N·m/rad
equivalent damping coefficient between the drill collar and drill bit	c_{cb}	181.49 N·m/rad
damping coefficient of drill bit	c_b	50 N·m/rad
coefficient of coulomb frication	μ_{cb}	0.5
coefficient of static friction	μ_{sb}	0.8
constant of Stribeck	γ_b	0.9
thickness of border stratum	D_v	0.000001 rad/s
radius of drill bit	R_b	0.155 m
WOB applied to the drill bit	W_{ob}	97,347 N
rotating torque	T_m	9400 Nm

The angular velocity results of the drill string stick–slip vibration simulation in this study are shown in Figure 3. The subscripts *r*, *p*, *l*, and *b* of angular velocity represent the rotary table, drill pipe, drill collar, and drill bit, respectively.

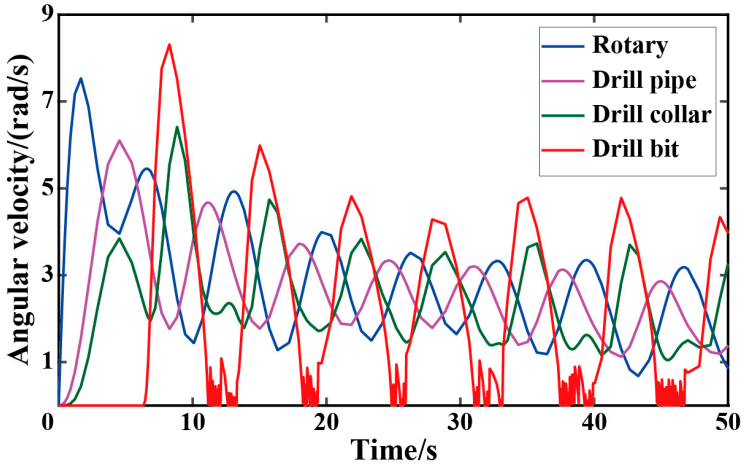

Figure 3. Simulation block diagram of drill string torsional vibration mode.

The angular velocity simulation results of drill string stick–slip vibration in this study have, overall, similar regular patterns to the simulation results in [18], with slight differences in details. The drill bit angular velocity in the stick section has slight fluctuations, while it is

completely 0 in [18]. The variation regular patterns of the rotary table, drill pipe, and drill collar are identical, exhibiting angular velocities generated in sequence with decreasing initial wave crests. Therefore, the drill string stick–slip vibration simulation research in this study is reliable and effective.

3.2. Analysis of Stick–Slip Vibration Characteristics

Based on the established drill string stick–slip vibration model simulation, the time domain variations of drill bit angular displacement, angular velocity, and angular acceleration at 9400 N·m rotary table torque are shown in Figure 4. For a clear description of typical stick–slip patterns, an image was drawn over 30 s.

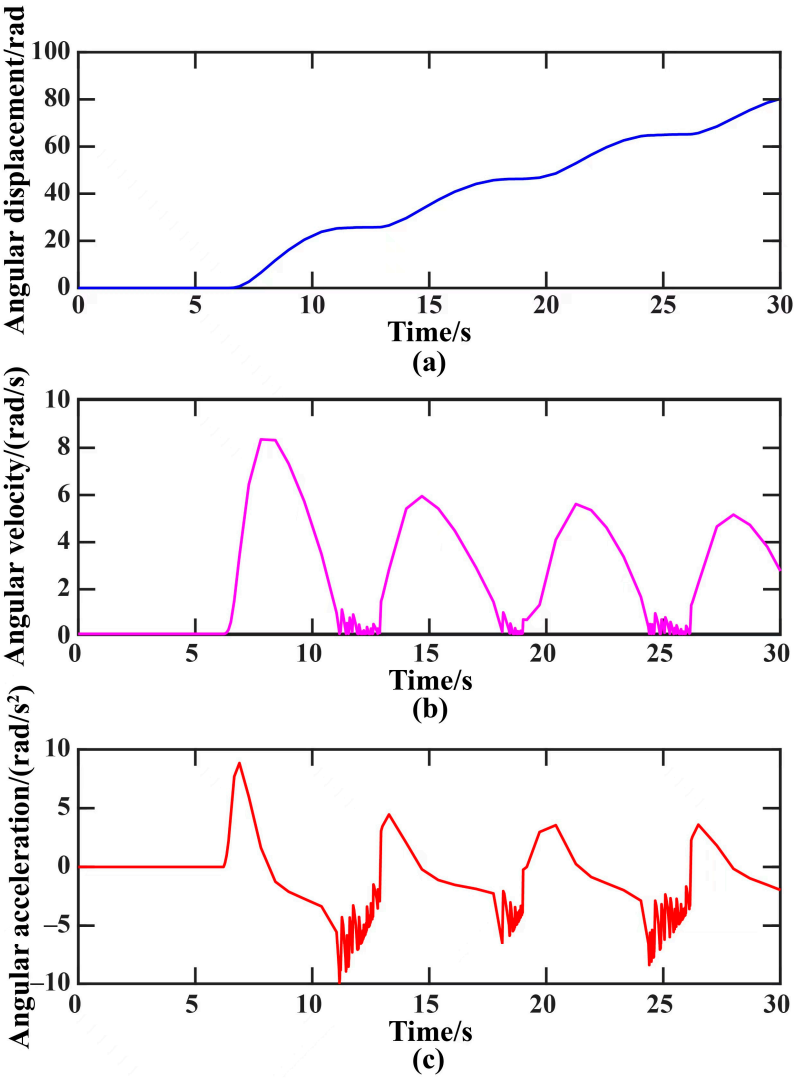

Figure 4. Time domain diagram of drill bit angular displacement, angular velocity, and angular acceleration. (**a**) drill bit angular displacement; (**b**) angular velocity; (**c**) angular acceleration.

Figure 4 shows the time domain graphs of drill bit angular displacement, angular velocity, and angular acceleration. When applying a 9.4 kN·m rotary table torque, the drill bit experiences three stages: stationary, slip, and stick. From 0 to 6.2 s, the drill bit is in the stationary stage with 0 angular displacement, velocity, and acceleration, as shown in Figure 4a–c. The drill bit needs to overcome the stiction torque. It can be seen from 6.2 to 11.2 s in Figure 4a–c that the drill bit is in the slip stage, which can be divided into three periods. Early slip period: The accumulated torque in the drill string is suddenly released, and the angular acceleration of the drill bit begins to increase dramatically. When

the torque is fully released, the angular acceleration reaches its maximum, so the angular velocity increases rapidly. Middle slip period: The drill bit is then mainly affected by the formation friction. The angular acceleration starts to decrease. When the drill string torque balances the formation friction torque, the angular acceleration is 0, and the angular velocity reaches its maximum, so the angular displacement increases fastest. Late slip period: Due to the formation friction, the angular acceleration starts to increase in the opposite direction, as shown in Figure 4c. The angular velocity quickly decreases to 0, so the angular displacement is also 0. From 11.2 to 12.9 s, when entering the stick stage, the drill bit angular velocity experiences slight changes of small magnitude belonging to minor fluctuations, as shown in Figure 4b. The angular displacement barely changes, as shown in Figure 4a. After breaking through the stationary stage, continuous and stable slip and stick stages occur, forming a stable stick–slip behavior in the drill string.

When the drill string exhibits stick–slip behavior, the angular velocity response of the rotary table, drill pipe, drill collar, and drill bit in the multidimensional drill string torsional vibration model is analyzed. Figure 5 shows the time domain graphs of the angular velocities of the four lumped masses.

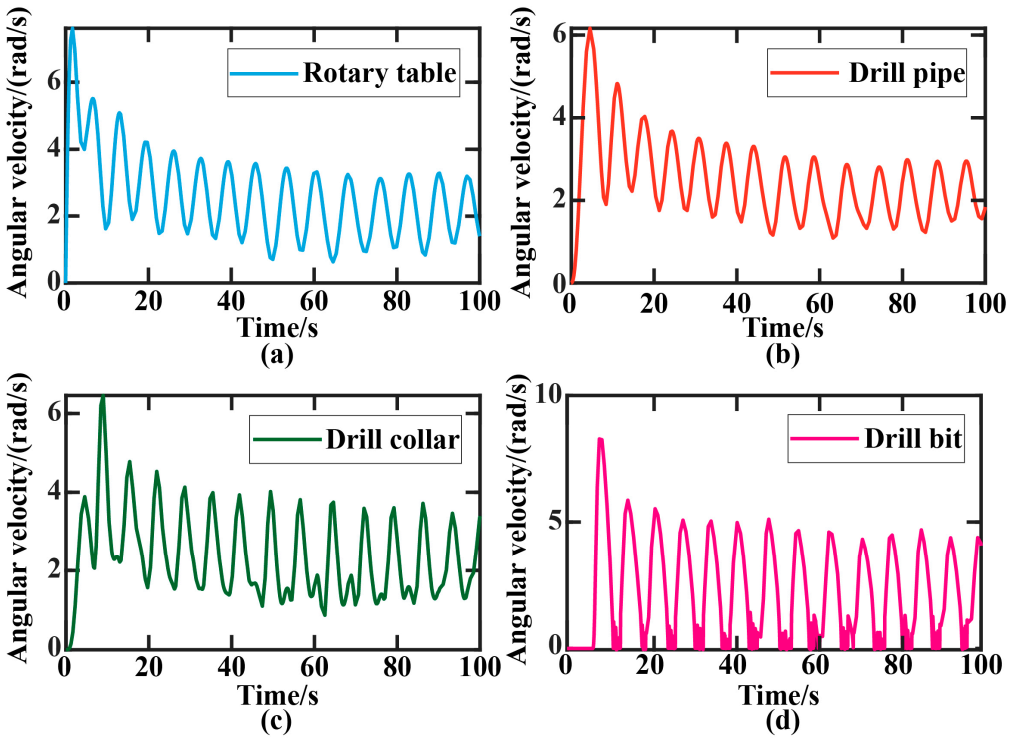

Figure 5. Time diagram of drill tool angular velocity during stick–slip vibration of drill string. (**a**) rotary table; (**b**) drill pipe; (**c**) drill collar; (**d**) drill bit.

It can be seen from Figure 5 that when the drill bit in Figure 5d exhibits stick–slip behavior, its angular velocity shows periodical fluctuations. The rotary table in Figure 5a, drill pipe in Figure 5b, and drill collar in Figure 5c also exhibit periodical fluctuations accordingly. When the drilling rig overcomes the stationary stage, the rotary table, drill pipe, drill collar, and drill bit generate angular velocities in sequence. So, there is a displacement lag between the drill bit and rotary table. Continuing to study their angular displacement regular patterns, the time domain variations of angular displacement are as follows.

It can be seen from Figure 6 that the rotary in Figure 6a starts rotating at 1 s, the drill pipe in Figure 6b at 2 s, the drill collar in Figure 6c at 2.7 s, and the drill bit in Figure 6d at 7 s. This is because the drill bit is also under the dry friction torque between the bit and th

rock. At this time, the drill bit angular displacement already lags behind the rotary table by 36.5 rad.

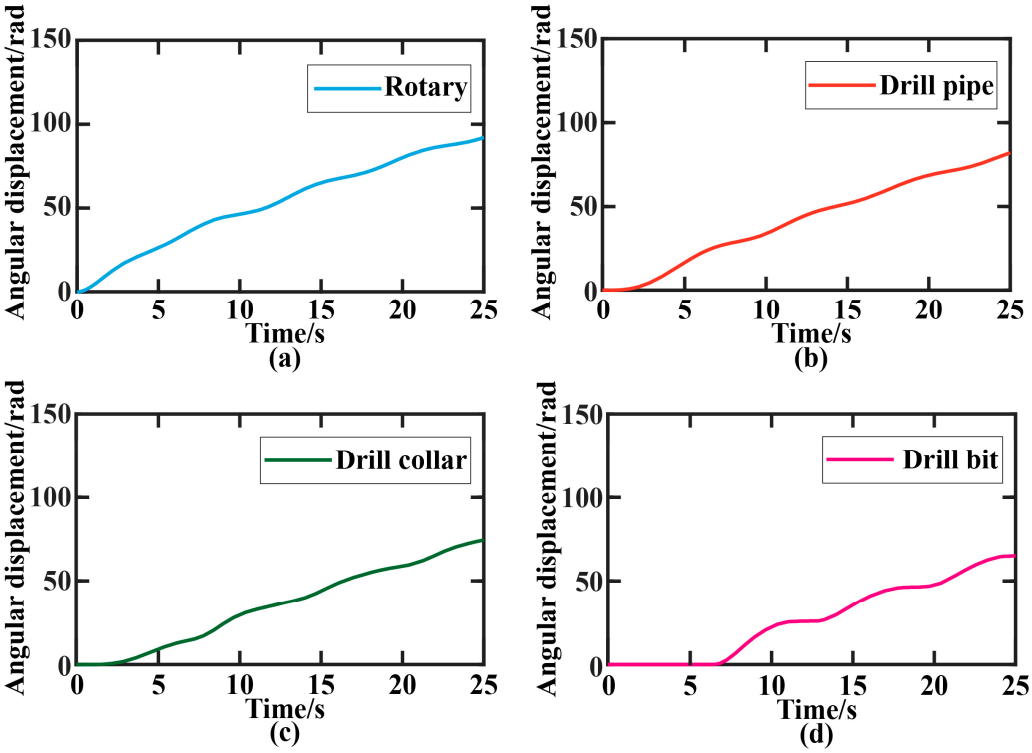

Figure 6. Time diagram of drill tool angular displacement during stick–slip vibration. (**a**) rotary; (**b**) drill pipe; (**c**) drill collar; (**d**) drill bit.

3.3. Analysis of Influencing Factors

As the rotary table torque increases, the drill string exhibits five different phenomena: the drill bit always sticking, minor stick–slip, typical stick–slip, stick–slip stability, and no stick–slip stability. To study the specific impact of rotary table torque on the typical stick–slip characteristics of the drill string, the typical stick–slip section is selected for further study. Based on example simulations, rotary table torques are set to 9000 N·m, 9200 N·m, 9300 N·m, 9400 N·m, and 9600 N·m, respectively. WOB is set to 97,347 N during the calculation. The time domain variations of drill bit angular velocity are obtained as follows.

Setting the rotary table speeds to 1 rad/s, 3 rad/s, 5 rad/s, and 7 rad/s, respectively, WOB is 97,347 N, and the torque is 9400 N·m during the calculation. The time domain variations of drill bit angular velocity are obtained as follows.

Taking the 9400 N·m rotary table torque, resulting in stick–slip behavior as a baseline, WOB is set to 97,000 N, 99,000 N, 100,000 N, and 110,000 N, respectively. The time domain variations of drill bit angular velocity are obtained as follows.

Analyzing the relatively stable stick–slip behavior of the drill string from 50 s to 100 s, shown in Figures 7–9, it can be seen that when the drill string exhibits stick–slip, the larger the rotary table torque, rotary speed, or WOB, the shorter the stick–slip period and stick duration. The drill bit angular velocity departs from the zero point sooner. The peak angular velocity of the drill bit becomes larger and larger. The angular velocity of the drill bit is greater. Moreover, the ratio of drill bit to rotary table angular velocity decreases as rotary table torque, speed, or WOB increases. The ratio is 1 without stick–slip.

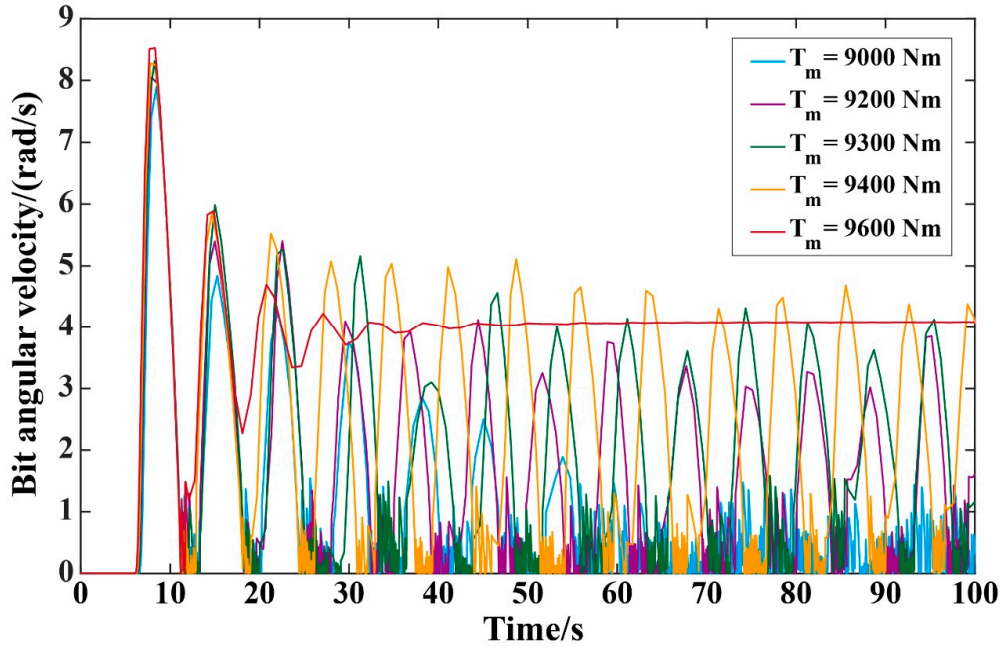

Figure 7. Time domain diagram of drill bit angular velocity with different turntable torque.

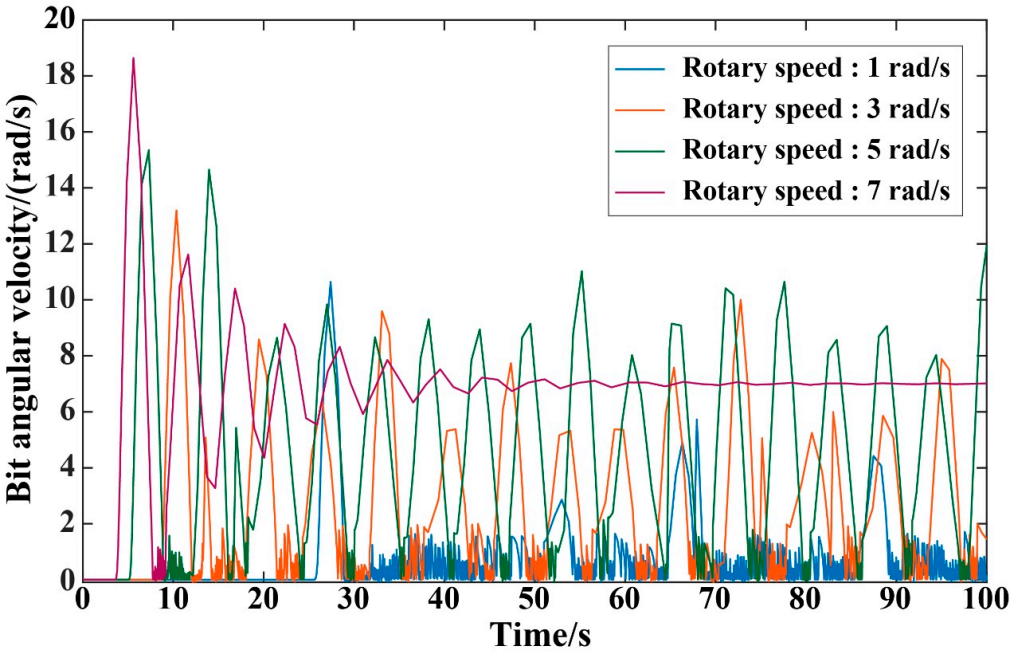

Figure 8. Time domain diagram of drill bit angular velocity at different turntable speeds.

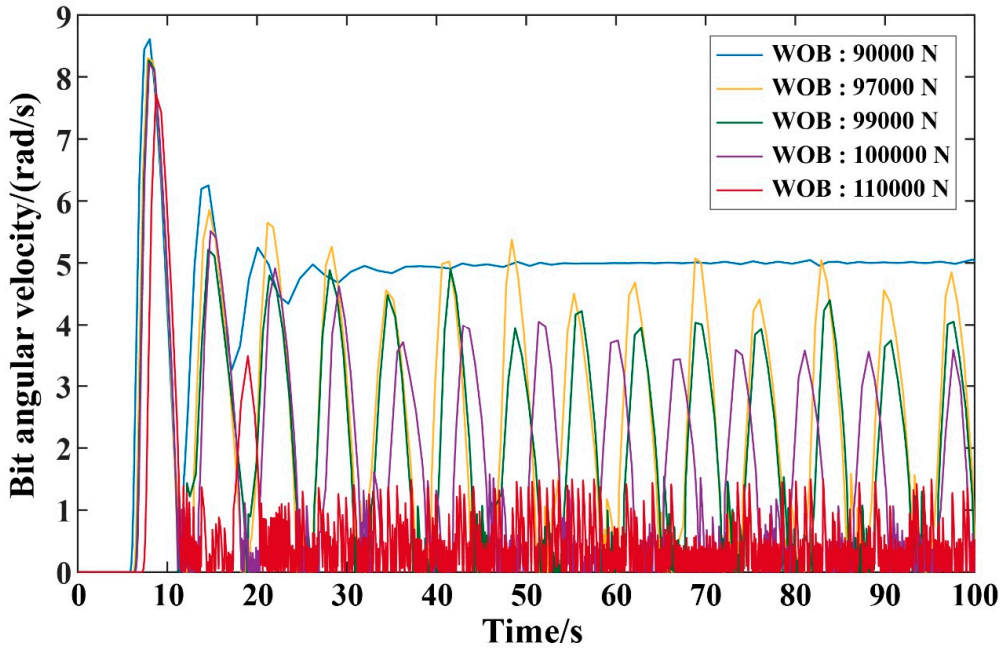

Figure 9. Time domain diagram of bit angular velocity at different weight-on-bit.

4. Case Study of the Stick–Slip-Model-Based Drilling Parameters Optimization

4.1. Drilling Parameter Optimization for Soft, Medium-Hard, and Hard Formations

The drillability of soft formation rating is set as 4.19, with the main rocks being mudstone, sandstone, and pebbled sandstone. Based on the rock friction coefficient table, the dynamic friction coefficient is 0.15, and maximum static friction coefficient is 0.4. The medium-hard formation simulates siliceous limestone with a rock drillability rating of 7. Its dynamic friction coefficient is 0.35, and maximum static friction coefficient is 0.6. In drilling parameter optimization for the hard formation, quartzite is simulated with a rock drillability rating of 11. Its dynamic friction coefficient is 0.45, and maximum static friction coefficient is 0.7. Parameters required for the ROP of the three formations are shown in Table 2.

Table 2. Parameter table of ROP in 3 kinds of formations.

Parameter Description	Parameter Symbol	Soft Formation	Medium-Hard Formation	Hard Formation
threshold weight	M	10 kN	20 kN	30 kN
rotate speed index	λ	0.68	0.68	0.68
tooth wear coefficient	C_2	3.26	3.82	4.68
pressure difference influence coefficient	C_p	1	1	1
water purification coefficient	C_h	1	1	1
tooth wear	h	0.7	0.75	0.8
formation drillability coefficient	K_R	0.0038	0.0020	0.0008

In the soft formation, the torque is 3 kN·m, and WOB is 93 kN when drill string torsional vibration occurs. Taking these as initial values, equal intervals are divided. Torque is increased by 0.3 kN·m each time, and WOB is decreased by 7 kN each time. In the medium-hard formation, the initial torque is 5 kN·m, and WOB is 93 kN during drill string torsional vibration. Torque is increased by 0.3 kN·m each time, and WOB is decreased by 4 kN each time. In the hard formation, the initial torque is 6 kN·m, and WOB is 93 kN during drill string torsional vibration. Torque is increased by 0.3 kN·m each time, and WOB is decreased by 4 kN each time. The vibration state and ROP of the drill string under different drilling parameters in the three formations can be obtained. If the drill string is

always in stick–slip vibration, the ROP fluctuates periodically and is marked as stick–slip. If stick–slip vibration disappears after a period, the ROP is obtained, in m/h, as shown in Tables 3–5.

Table 3. Table of optimization results of drilling parameters for softer formations.

WOB (kN) \ Torque (kN·m)	3	3.3	3.6	3.9	4.2	4.5
93	stick–slip	stick–slip	stick–slip	stick–slip	1.44	1.56
86	stick–slip	stick–slip	stick–slip	1.26	1.36	1.46
79	stick–slip	stick–slip	stick–slip	1.18	1.27	1.36
72	stick–slip	stick–slip	1.01	1.09	1.17	1.25
65	stick–slip	0.84	0.92	1.00	1.07	1.14
58	0.69	0.76	0.83	0.89	0.96	1.01

Table 4. Optimal result table of drilling parameters for medium-hard formations.

WOB (kN) \ Torque (kN·m)	5.0	5.3	5.6	5.9	6.2	6.5
93	stick–slip	stick–slip	stick–slip	stick–slip	0.57	0.61
89	stick–slip	stick–slip	stick–slip	stick–slip	0.56	0.60
85	stick–slip	stick–slip	stick–slip	0.50	0.54	0.58
81	stick–slip	stick–slip	0.46	0.49	0.53	0.56
77	stick–slip	0.41	0.44	0.48	0.51	0.54
73	0.36	0.40	0.43	0.46	0.49	0.52

Table 5. Table of optimization results of drilling parameters for hard formations.

WOB (kN) \ Torque (kN·m)	6.0	6.3	6.6	6.9	7.2	7.5
93	stick–slip	stick–slip	stick–slip	stick–slip	0.159	0.171
89	stick–slip	stick–slip	stick–slip	0.144	0.157	0.168
85	stick–slip	stick–slip	stick–slip	0.142	0.153	0.163
81	stick–slip	stick–slip	0.128	0.138	0.148	0.157
77	stick–slip	0.115	0.124	0.133	0.142	0.150
73	0.102	0.111	0.119	0.127	0.135	0.142

It can be seen from Table 3 that in the soft formation, with the goals of eliminating drill string stick–slip vibration and having an ROP greater than 1.40 m/h, there are three solutions in the table. When torque is increased to above 4.2 kN and WOB can be reduced to 86 kN, the ROPs are 1.44 m/h, 1.46 m/h, and 1.56 m/h, respectively. From Table 4, in the medium-hard formation, with the goals of eliminating drill string stick–slip vibration and having an ROP greater than or equal to 0.57 m/h, there are four solutions in the table. When torque is increased to above 6.2 kN and WOB can be reduced to 85 kN, the ROPs are 0.57 m/h, 0.58 m/h, 0.60 m/h, and 0.61 m/h, respectively. From Table 5 it can be seen that in the hard formation, with the goals of eliminating stick–slip vibration and having an ROP greater than or equal to 0.159 m/h, there are four solutions in the table. When torque is increased to above 7.2 kN and WOB can be reduced to 85 kN, the ROPs are 0.159 m/h, 0.163 m/h, 0.168 m/h, and 0.171 m/h, respectively.

The soft formation has three optimization solutions; the medium-hard and hard formations have four. The ROP time domain graphs are compared in Figures 10–12.

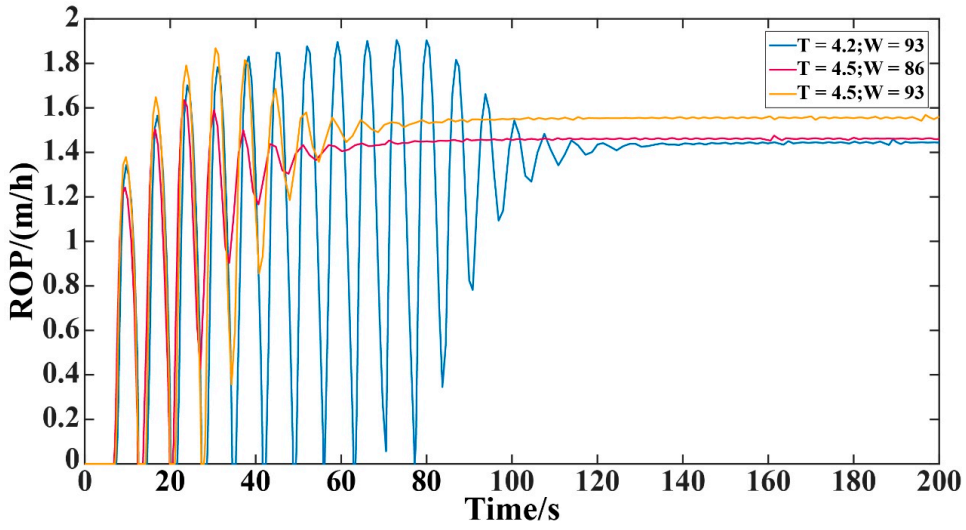

Figure 10. Time domain diagram of drilling speed optimization for soft formations.

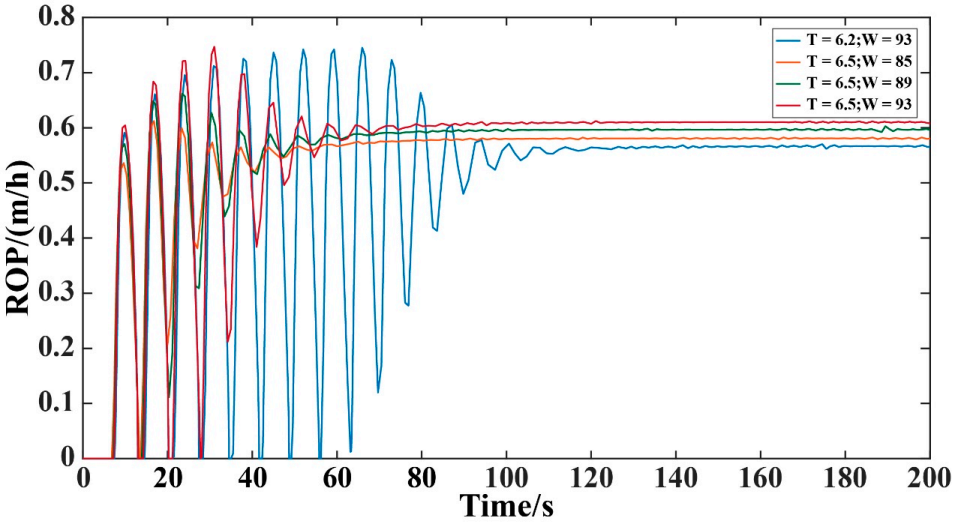

Figure 11. Time domain diagram of drilling speed optimization for medium-hard formations.

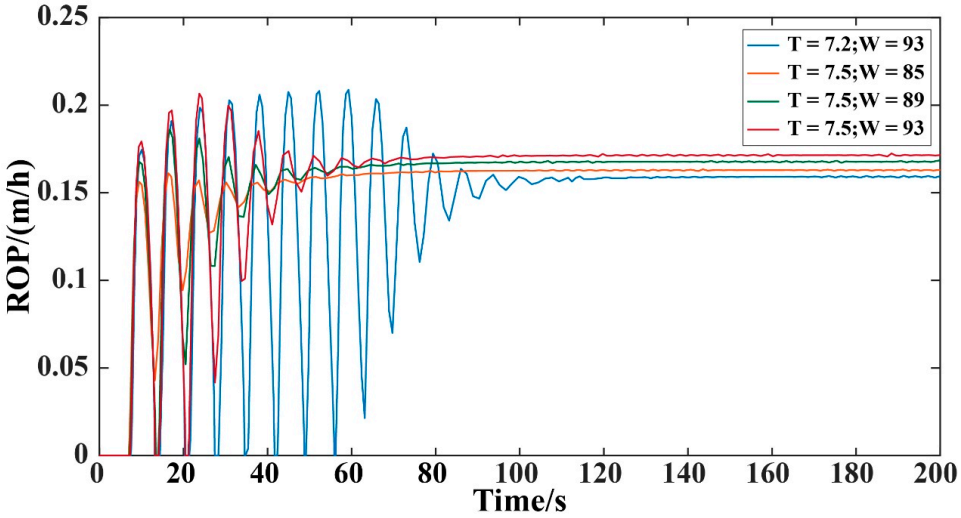

Figure 12. Time domain diagram of mechanical drilling rate optimization for drilling parameters in hard formations.

4.2. Comparison of the Optimized Results

In order to minimize the adjustments, among the three solutions for the soft formation, the WOB of 93 kN and torque of 4.2 kN·m were selected as the optimal drilling parameters for this formation. Among the four solutions for the medium-hard formation, the WOB of 93 kN and torque of 6.2 kN·m were selected as the optimal drilling parameters. Among the four solutions for the hard formation, the WOB of 93 kN and torque of 7.2 kN·m were selected as the optimal drilling parameters. The drill bit vibration effects and ROP without and with optimization of the drilling parameters for the three formations were then compared, as shown in Figures 13–15.

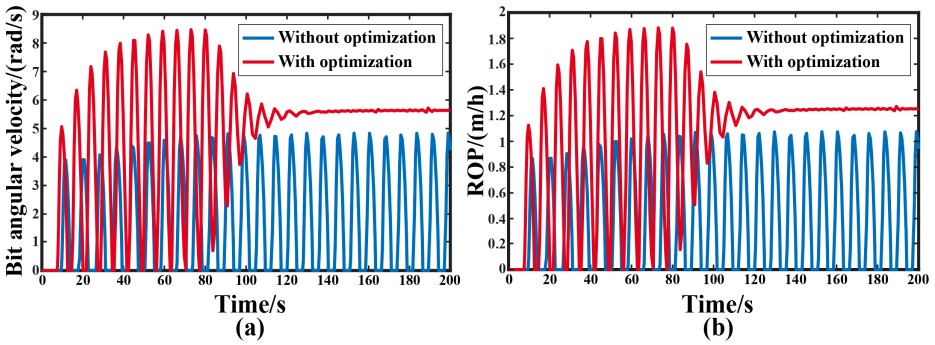

Figure 13. Diagram of bit angular velocity optimization of drilling parameters in soft formation. (**a**) bit angular velocity; (**b**) ROP.

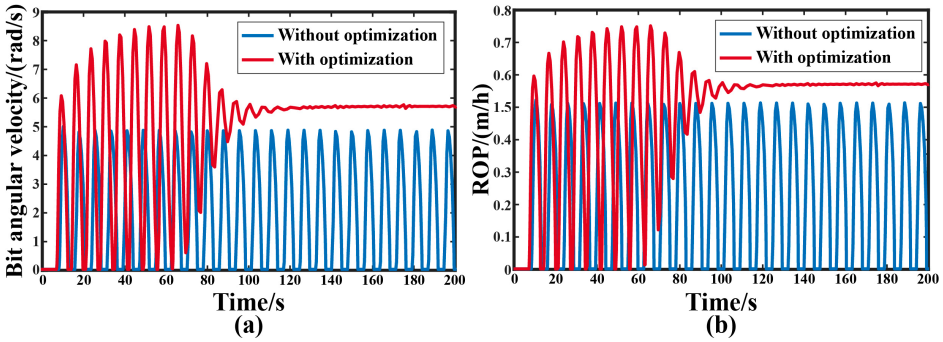

Figure 14. Diagram of bit angular velocity optimization of drilling parameters in medium-hard formation. (**a**) bit angular velocity; (**b**) ROP.

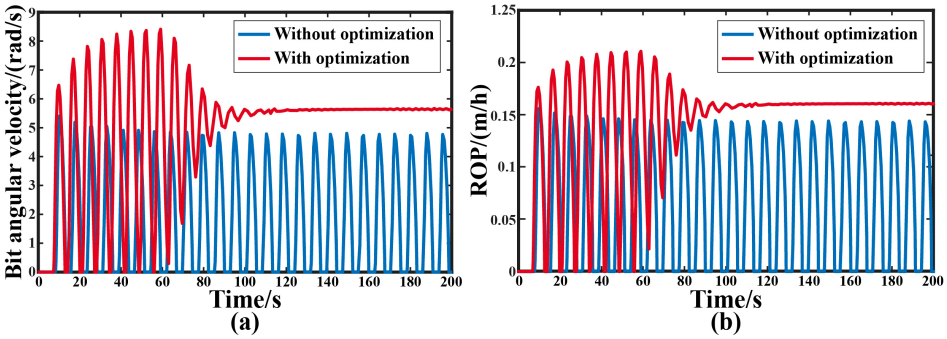

Figure 15. Diagram of bit angular velocity optimization of drilling parameters in hard formation. (**a**) bit angular velocity; (**b**) ROP.

Figure 13 shows that in the soft formation, without optimization of the drilling parameters, the drill string experienced steady stick–slip vibration. The peak value of the drill bit angular velocity was about 4.8 rad/s, as shown in Figure 13a, and the ROP fluctuated

periodically with a peak value of approximately 1.3 m/h, as shown in Figure 13b. With optimization of the drilling parameters, the drill string experienced 125 s of stick–slip vibration. During this stage, the maximum drill bit angular velocity was about 8.4 rad/s, as shown in Figure 13a, and the maximum ROP was about 1.9 m/h, as shown in Figure 13b. After that, stick–slip vibration no longer occurred. The drill bit angular velocity was about 5.6 rad/s, and the ROP was about 1.45 m/h. This indicates that through optimization of the drilling parameters, after 125 s, the drill string no longer experienced stick–slip vibration. The drill bit angular velocity increased by 16.7%, and the ROP increased by 11.5%.

Figure 14 shows that in the medium-hard formation, without optimization of the drilling parameters, the drill string experienced steady stick–slip vibration. The peak value of the drill bit angular velocity was about 4.9 rad/s, as shown in Figure 14a, and the ROP fluctuated periodically with a peak value of approximately 0.51 m/h, as shown in Figure 14b. With optimization of the drilling parameters, the drill string experienced 110 s of stick–slip vibration. During this stage, the maximum drill bit angular velocity was about 8.2 rad/s, as shown in Figure 14a, and the maximum ROP was about 0.74 m/h, as shown in Figure 14b. After that, stick–slip vibration no longer occurred. The drill bit angular velocity was about 5.6 rad/s, and the ROP was about 0.57 m/h. This indicates that through optimization of the drilling parameters, after 110 s, the drill string no longer experienced stick–slip vibration. The drill bit angular velocity increased by 14.3%, and the ROP increased by 13.7%.

Figure 15 shows that in the hard formation, without optimization of the drilling parameters, the drill string experienced steady stick–slip vibration. The peak value of the drill bit angular velocity was about 4.8 rad/s, as shown in Figure 15a, and the ROP fluctuated periodically with a peak value of approximately 0.14 m/h, as shown in Figure 15b. With optimization of the drilling parameters, the drill string experienced 105 s of stick–slip vibration. During this stage, the maximum drill bit angular velocity was about 8.3 rad/s, as shown in Figure 15a, and the maximum ROP was about 0.21 m/h, as shown in Figure 15b. After that, stick–slip vibration no longer occurred. The drill bit angular velocity was about 5.6 rad/s, and the ROP was about 0.16 m/h. This indicates that through optimization of the drilling parameters, after 105 s, the drill string no longer experienced stick–slip vibration. The drill bit angular velocity increased by 16.7%, and the ROP increased by 14.3%.

5. Conclusions

Based on the drill string torsional vibration model, this paper established and validated a drill string stick–slip vibration condition model and revealed the characteristics of drill string stick–slip vibration. It was found that the drill bit periodically changes between stationary, slip, and stick stages, and the angular velocity in the slip stage is much greater than that in the stick stage. When stick–slip vibration occurred in the drill string, there was significant displacement lag and torque fluctuation between the drill bit and rotary. The analysis showed that the higher the rotary torque, rotate speed, and WOB, the shorter the period and the greater the amplitude of the stick–slip vibration. On this basis, the relationship between torque, WOB, and ROP was established, and drilling parameter optimization was completed for soft, medium-hard, and hard formations. The results showed that appropriately increasing torque and reducing WOB can effectively reduce or even eliminate stick–slip vibration of the drill string and improve the ROP. Parameter optimization in the soft formation improved ROP by 11.5%, in the medium-hard formation by 13.7%, and in the hard formation by 14.3%. This provides theoretical guidance for field operations and has important engineering application value.

Author Contributions: Conceptualization, C.W. and Z.W.; methodology, C.W.; software, Z.W.; validation, J.L. and G.L.; formal analysis, C.W.; investigation, Z.W.; resources, Z.W.; data curation, Z.W.; writing—original draft preparation, C.W.; writing—review and editing, W.C.; visualization, W.C.; supervision, J.L.; project administration, C.W.; funding acquisition, C.W. All authors have read and agreed to the published version of the manuscript.

Funding: This research was funded by The Major Scientific Research Instrument Development Program of National Natural Science Foundation of China grant number No. 52227804 and National Natural Science Foundation of China grant number No. 52304001.

Data Availability Statement: Data is unavailable due to privacy or ethical restrictions.

Conflicts of Interest: The authors declare no conflict of interest.

References

1. Yigit, A.; Christoforou, A. Coupled torsional and bending vibrations of actively controlled drillstrings. *J. Sound Vib.* **2000**, *234*, 67–83. [CrossRef]
2. Eronini, I.; Somerton, W.; Auslander, D. A dynamic model for rotary rock drilling. *J. Energy Resour. Technol.* **1982**, *104*, 108–120. [CrossRef]
3. Richard, T.; Germay, C.; Detournay, E. Self-excited stick–slip oscillations of drill bits. *Comptes Rendus Mécanique* **2004**, *332*, 619–626. [CrossRef]
4. Besselink, B.; Van De Wouw, N.; Nijmeijer, H. A semi-analytical study of stick-slip oscillations in drilling systems. *J. Comput. Nonlinear Dyn.* **2011**, *6*, 021006. [CrossRef]
5. Khulief, Y.; Al-Sulaiman, F.; Bashmal, S. Vibration analysis of drillstrings with self-excited stick–slip oscillations. *J. Sound Vib.* **2007**, *299*, 540–558. [CrossRef]
6. Germay, C.; Van De Wouw, N.; Nijmeijer, H.; Sepulchre, R. Nonlinear Drillstring Dynamics Analysis. *SIAM J. Appl. Dyn. Syst.* **2009**, *8*, 527–553. [CrossRef]
7. Leine, R.; Van Campen, D.; Keultjes, W. Stick-slip whirl interaction in drillstring dynamics. *J. Vib. Acoust.* **2002**, *124*, 209–220. [CrossRef]
8. Jansen, J.D.; Van Den Steen, L. Active damping of self-excited torsional vibrations in oil well drillstrings. *J. Sound Vib.* **1995**, *179*, 647–668. [CrossRef]
9. Puebla, H.; Alvarez-Ramirez, J. Suppression of stick-slip in drillstrings: A control approach based on modeling error compensation. *J. Sound Vib.* **2008**, *310*, 881–901. [CrossRef]
10. Navarro-Lopez, E.M.; Cortes, D. Sliding-Mode Control of a Multi-DOF Oilwell Drillstring with Stick-Slip Oscillations. In Proceedings of the 2007 American Control Conference, New York, NY, USA, 9–13 July 2007.
11. Canudas-De-Wit, C.; Rubio, F.R.; Corchero, M.A. D-OSKIL: A New Mechanism for Controlling Stick-Slip Oscillations in Oil Well Drillstrings. *IEEE Trans. Control Syst. Technol.* **2008**, *16*, 1177–1191. [CrossRef]
12. Navarro-López, E.M.; Cortés, D. Avoiding harmful oscillations in a drillstring through dynamical analysis. *J. Sound Vib.* **2007**, *307*, 152–171. [CrossRef]
13. Zamanian, M.; Khadem, S.E.; Ghazavi, M. Stick-slip oscillations of drag bits by considering damping of drilling mud and active damping system. *J. Pet. Sci. Eng.* **2007**, *59*, 289–299. [CrossRef]
14. Yigit, A.S.; Christoforou, A.P. Stick-slip and bit-bounce interaction in oil-well drillstrings. *J. Energy Resour. Technol.* **2006**, *128*, 268–274. [CrossRef]
15. Lin, Y.-Q.; Wang, Y.-H. Stick-slip vibration of drill strings. *J. Eng. Ind.* **1991**, *113*, 38–43. [CrossRef]
16. Richard, T.; Germay, C.; Detournay, E. A simplified model to explore the root cause of stick–slip vibrations in drilling systems with drag bits. *J. Sound Vib.* **2007**, *305*, 432–456. [CrossRef]
17. Richard, T.; Detournay, E. Stick–slip motion in a friction oscillator with normal and tangential mode coupling. *Comptes Rendus De L'Académie Des Sci.-Ser. IIB-Mech.* **2000**, *328*, 671–678. [CrossRef]
18. Navarro-López, E.M.; Licéaga-Castro, E. Non-desired transitions and sliding-mode control of a multi-DOF mechanical system with stick-slip oscillations. *Chaos Solitons Fractals* **2009**, *41*, 2035–2044. [CrossRef]
19. Kyllingstad, Å.; Halsey, G. A study of slip/stick motion of the bit. *SPE Drill. Eng.* **1988**, *3*, 369–373. [CrossRef]
20. Krama, A.; Gharib, M.; Refaat, S.S.; Sassi, S. Hybrid fuzzy sliding mode for stick-slip suppression in drill string systems. *J. Mech. Sci. Technol.* **2022**, *36*, 1089–1102. [CrossRef]
21. Liu, J.; Wang, J.; Guo, X.; Dai, L.; Zhang, C.; Zhu, H. Investigation on axial-lateral-torsion nonlinear coupling vibration model and stick-slip characteristics of drilling string in ultra-HPHT curved wells. *Appl. Math. Model.* **2022**, *107*, 182–206. [CrossRef]
22. MacLean, J.D.; Vaziri, V.; Aphale, S.S.; Wiercigroch, M. Suppressing stick–slip oscillations in drill-strings by Modified Integral Resonant Control. *Int. J. Mech. Sci.* **2022**, *228*, 107425. [CrossRef]
23. Riane, R.; Doghmane, M.Z.; Kidouche, M.; Djezzar, S. Observer-Based H Controller Design for High Frequency Stick-Slip Vibrations Mitigation in Drill-String of Rotary Drilling Systems. *Vibration* **2022**, *5*, 264–289. [CrossRef]
24. Taraghi Osguei, A.; Mohammad Alizadeh, B.; Dobakhti, A. Two-three degree of freedom model for Anti Stick-Slip Tool of Drill-string. *Amirkabir J. Mech. Eng.* **2023**, *55*, 4.
25. Long, Y.; Wang, X.; Wang, P.; Zhang, F. A Method of Reducing Friction and Improving the Penetration Rate by Safely Vibrating the Drill-String at Surface. *Processes* **2023**, *11*, 1242. [CrossRef]

26. Rill, G.; Schuderer, M. A Second Order Dynamic Friction Model Compared to Commercial Stick-Slip Models. *Modelling* **2023**, *4*, 366–381. [CrossRef]
27. Guan, Z.; Chen, T.; Liao, H. *Theory and Technology of Drilling Engineering*; Springer: Berlin, Germany, 2021.